Deoxynivalenol induces apoptosis and inflammation in the liver: Analysis using precision-cut liver slices

Amanda Lopes Hasuda, Elodie Person, Abdullah Khan Khoshal, Sandrine Bruel, Sylvie Puel, Isabelle P. Oswald, Ana Paula F.R. L. Bracarense, Philippe Pinton

Deoxynivalenol induces apoptosis and inflammation in the liver: analysis using precision-cut liver slices

Amanda Lopes Hasuda[1,2*], Elodie Person[2], Abdullah Khan Khoshal[2], Sandrine Bruel[2], Sylvie Puel[2], Isabelle P. Oswald[2*], Ana Paula F. R. L. Bracarense[1], Philippe Pinton[2]

[1] Laboratory of Animal Pathology, Universidade Estadual de Londrina, P.O. Box 10.011, Londrina, PR 86057-970, Brazil; amanda.lopeshasuda@uel.br (A.L.H.) anapaula@uel.br (A.P.B.)

[2] Toxalim (Research Centre in Food Toxicology), University of Toulouse, INRAE, ENVT, INP-Purpan, UPS, 31027, Toulouse, France; elodie.person@inrae.fr (E.P.), a.khoshal@outlook.com (A.K.), sandrine.bruel@inrae.fr (S.B.), sylvie.puel@inrae.fr (S.P.); isabelle.oswald@inrae.fr (I.P.O.); philippe.pinton@inrae.fr (P.P.)

[*]Corresponding authors: amanda.lopeshasuda@uel.br, isabelle.oswald@inrae.fr

Received: date; Accepted: date; Published: date

ABSTRACT

Deoxynivalenol (DON) is one of the most common mycotoxins in cereals and their by-products. Its adverse effects on animal and human health have been extensively studied in the intestine, but little attention has been paid to another target organ for mycotoxins, the liver that is potentially exposed after intestinal absorption and enterohepatic circulation. To assess DON's toxicity in an *ex vivo* model structurally and physiologically closer to the whole liver, we developed a pig precision-cut liver slices (PCLS) model. PCLS contain all cell types and maintain intercellular and cell-matrix interactions, among other architectural features of the liver. The human HepG2 cell line was used for comparison. We observed that after a short exposure, DON reduced the cell viability of HepG2 cells and induced the expression of genes involved in apoptosis, inflammation and oxidative stress. When PCLS were exposed to DON, damage to the tissues was observed, with no changes in markers of liver function or injury. Exposure to the toxin also triggered liver inflammation and apoptosis, effects already observed in pigs fed DON-contaminated diets. Overall, these data demonstrate that DON had toxic effects on a liver cell line and on whole liver tissue,

consistent with the effect observed during *in vivo* exposure. They also indicate that pig PCLS is a relevant and sensitive model to investigate the liver toxicity of food contaminants.

Keywords: cell death, liver, explants, histology, inflammation, apoptosis, mycotoxins

1. INTRODUCTION

Mycotoxins are toxic secondary metabolites produced by fungi, mainly by *Aspergillus, Penicillium, Alternaria, Fusarium* and *Claviceps*. They are the most frequently occurring natural contaminants in human food and in animal feed. They are highly resistant to a range of food processes including cooking and therefore end up on our plates (Payros et al., 2021a). Estimates show that 60-80% of food crops worldwide are contaminated with these toxins (Eskola et al., 2020).

Among mycotoxins, deoxynivalenol (DON) is the most prevalent member of the trichothecene family. It is mainly produced by *Fusarium graminearum and F. culmorum* (Knutsen et al., 2017). In Europe, DON was detected in almost half of 26,613 cereal samples collected from 21 countries, with the highest levels observed in wheat, maize and oat grains (Knutsen et al., 2017). Similarly, in the southern region of Brazil, one of the largest crops producing regions, 48% of the maize samples analyzed were contaminated with this toxin (Oliveira et al., 2017).

In 2017, EFSA set a tolerable daily intake (TDI) of 1 µg/kg of body weight/day for the sum of DON and its modified forms (Knutsen et al., 2017). Data obtained at the European and national levels indicate that this TDI may be exceeded in some parts of the population, particularly children (Knutsen et al., 2017; Narváez et al., 2022; Vin et al., 2020), indicating that exposure to DON is of concern for humans.

At the molecular level, DON binds to the 60S ribosomal subunit, inducing ribotoxic stress, inhibiting protein synthesis and activating mitogen-activated protein kinases and their downstream pathways (Pestka, 2010a). Vomiting and bloody diarrhea have been reported following acute exposure to DON (Pestka, 2010b; Ruan et al., 2020). Chronic exposure to the toxin reduces food consumption and weight gain and induces neuroendocrine changes (Payros et al., 2016; Terciolo et al., 2018), alteration of the immune system (Pinton et al., 2008), and disturbance of intestinal morphology and functions (Pinton and Oswald, 2014; Robert et al., 2017).

The effect of DON on the liver is poorly described, even though it can be a target for mycotoxins. The functional capacities of this organ are mainly related to anabolic and catabolic processes including energy metabolism and xenobiotics detoxification, storage and circulation of nutrients, as well as protein synthesis and bile production. *In vitro* studies with human hepatic cells lines have focused on cytotoxicity, apoptotic and transcription factors (Fernández-Blanco et al., 2018; Mayer et al., 2017; Smith et al., 2017a, 2017b; Zhang et al., 2009). The only study carried out on human primary hepatocytes demonstrated cytotoxicity, decreased albumin secretion and increased apoptosis (Königs et al., 2008). *In vivo* animal trials showed that ingestion of DON targets the liver; oral exposure to the toxin alters the liver morphology, induces an inflammatory response, increases apoptosis and oxidative stress (Bracarense et al., 2017; Gerez et al., 2015; Grenier et al., 2011; Souza et al., 2020; Sun et al., 2014).

In the context of reducing the number of experimental animals (3Rs principles), *ex vivo* organ culture is a powerful model that preserves normal histological structure (Maresca et al., 2018). Indeed, large numbers of explants can be prepared from a single animal, thus reducing the number of animals and allowing multiple tests. The advantage of *ex vivo* approaches for the intestine has been demonstrated through observation of

reproducible toxic effects of mycotoxins, including DON (Alassane-Kpembi et al., 2017a, 2017b; Gerez et al., 2021; Pierron et al., 2022; Silva et al., 2019, 2014). Precision-cut liver slices (PCLS) are a physiologically relevant *ex vivo* model for hepatic studies (Palma et al., 2019). This model has features close to the *in vivo* situation, including the conservation of the complex 3D liver structure, as well as cell–cell and cell–matrix interactions. Moreover, PCLS provide the possibility to work with a complete multicellular liver model including hepatocytes, Kupffer cells, stellate cells, cholangiocytes and liver sinusoidal endothelial cells. As normal metabolism is necessary for morphological preservation, structural integrity is a valid criterion to demonstrate a successful culture (Starokozhko et al., 2015). Methodologies and parameters to produce and culture PCLS have been optimized over the past decades (de Graaf et al., 2010; Dewyse et al., 2021). It is now considered that PCLS provides a useful *ex vivo* tool to obtain multiple read-outs, and that it is relevant for studies investigating liver functionality, toxicity, chronic liver diseases and potential adverse effects on the immune system (Dewyse et al., 2021; Kasper et al., 2005; Wu et al., 2018). However, studies using *ex vivo* models from the liver are scarce and their advantages in analyzing the effects of mycotoxins remains to be demonstrated.

The objective of this work was thus to study the impact of DON on the liver using a liver slice model. In this model, histological damages, hepatic biomarkers and changes in gene expression were evaluated. HepG2 cells, which are widely used for hepatotoxicity studies, were used for comparison.

2. MATERIALS AND METHODS

2.1 Mycotoxin

DON was acquired from Sigma-Aldrich (Saint Quentin Fallavier, France), dissolved in dimethyl sulfoxide (DMSO) (Sigma-Aldrich), and stored at -20°C until use. Except for cytotoxicity assays, the DON working concentration was 10 µM, in accordance with our previous studies performed in different experimental models and tissues (Bracarense et al., 2020; Gerez et al., 2021, 2017).

2.2 In vitro assay

To evaluate DON hepatotoxicity and effects on gene expression, *in vitro* assays were performed using HepG2 cells, a human liver cancer cell line (Sigma, 85011430). Cells were maintained as previously described (Luo et al., 2019) for gene expression analysis. To assess the cytotoxicity, HepG2 cells were seeded in 96-white-well flat-bottom cell culture plates (Greiner, Courtaboeuf, France) (10^3 cells/well in 100 µL culture medium). After 24 h, the medium was replaced by a complete medium (without fetal calf serum) containing DON or vehicle (DMSO) and incubated for 4, 24, and 48 h. The cytotoxic effects of DON were determined by measuring the reducing potential of living cells and hence their metabolism, using the RealTime-Glo™ MT Cell Viability Assay (Promega, Charbonnières-les-Bains, France). Six biological replicates were performed.

For gene expression analysis, cells were incubated for 4 h with the mycotoxin or vehicle, lysed with Extract All (Eurobio, Les Ulis, France), and stored at -80°C prior to mRNA extraction. Six biological replicates were performed.

2.3 Preparation of liver slices

Animal experimentation procedures were approved by the Ethics Committee of Pharmacology-Toxicology of Toulouse-Midi-Pyrénées in animal experimentation

(Toxcométhique) (APAFIS#N2016080314392462), in accordance with the European Directive on the protection of animals used for scientific purposes.

Liver slices (PCLS) were prepared from liver lateral lobe resected from nine euthanized male 4–5-weeks-old piglets. The lobe was immediately flushed with an ice-cold sodium chloride solution (0.9% NaCl) to limit ischemia and remove hemoglobin.

To improve their viability during coring, slicing, and storage procedures, the liver slices were maintained in Krebs-Henseleit ice-cold buffer supplemented with $NaHCO_3$ (2.1 g/L) and $CaCl_2$, $2H_2O$ (0.373 g/L), previously bubbled with carbogen for 1 h. Eight-millimeter diameter cores were cut out and transferred to the Krumdieck tissue slicer (Alabama Research and Development, AL, USA) where 250 µm thick slices were cut (de Graaf et al., 2010). Damaged slices were discarded and perfect slices underwent homeostasis recovery during a 1 h regeneration step in ice-cold William's E Medium supplemented with 1% glutamine and 0.5% gentamycin (Eurobio) bubbled in carbogen. The slices were deposited in 12-wells culture plates (1 slice per well) for 4 h in 2 mL of complete William's E Medium previously bubbled in carbogen and containing 10 µM DON or vehicle. Incubation took place at 37°C under a 95% O_2 and 5% CO_2-controlled atmosphere.

After the incubation period, the cell culture medium was collected and frozen to detect hepatic injury markers. Some liver slices were snap-frozen and stored at -80°C until transcriptomic analyses. Others were fixed for 24 h in 4% buffered formaldehyde (VWR, Rosny-sous-Bois, France) and stored in 70% ethanol for histology and immunohistochemical experiments.

2.3.1 Histological evaluation

PCLS incubated for four hours were dehydrated in a series of alcohol solutions of increasing concentration and embedded in paraffin for histological examination. Sections of 5 µm were stained with hematoxylin and eosin (HE) and mounted with coverslips for histological analysis. A morphological lesion score as described by Terciolo et al. (2019) was used to evaluate histological changes in the liver. The extent of each lesion (according to the intensity or the frequency observed, scored from 0 to 3) and the severity factor were used to establish the lesion score scale (Table 1).

Table 1. Histological criteria used to establish liver lesion score.

Type of lesion	Severity factor	Maximal score
Disorganization of hepatic cords	1	33
Inflammatory infiltrate	1	
Cytoplasmic vacuolation	1	
Nuclear vacuolation	1	
Megalocytosis	2	
Apoptosis	2	
Necrosis	3	

The maximum lesion score was obtained by multiplying the lesion's maximum extent level by the organ's maximum severity factor. The lesion score was obtained by multiplying the severity factor by the extent of the lesion.

2.3.2 Hepatic biomarkers

To assess liver damage and function, hepatic enzyme activity and protein concentration were evaluated in the medium after a 4 h incubation period. Alanine transaminase (ALT), aspartate aminotransferase (AST), alkaline phosphatase (ALP), lactate dehydrogenase (LDH) activities and total protein (TP) concentrations were determined on a Pentra 400 chemistry analyzer (Horiba, Les Ulis, France) at the Anexplo Platform in Toulouse (France).

2.3.3 Immunohistochemical assessment of apoptosis

Apoptosis was assessed on liver slices by immunohistochemical analysis using the antibody anti-cleaved caspase-3 (CCasp3) (clone Asp 175, 1:200 dilution, Cell Signaling Technology, Beverly, MA) and the procedures previously described (Bracarense et al., 2017). Cells with positive immunostaining were counted in five random fields per section at 400x magnification, as described previously (Gerez et al., 2015).

2.4 Expression of mRNA encoding genes by real‐time qPCR

The RNA from tissue and cells was extracted as already described in (Grenier et al., 2012). The concentration and quality of the samples were analyzed, and reverse transcription and real-time qPCR were performed as previously described in (Maruo et al., 2018) using specific primers sequences purchased from Sigma (Tables 2 and 3). Most of the primers were specifically designed for this experiment.

2.4.1 Total RNA Extraction and Reverse Transcription

PCLS were lysed using 1 mL of Extract-All with ceramic beads (MP Biomedicals, Illkirch, France). Total RNA from PCLS and HepG2 assays were purified, and their concentration and integrity were determined as previously described (Maruo et al., 2018). For each sample, 2 µg of total RNA was reverse transcribed into cDNA and diluted 1:20 with nuclease-free/injection water (Ambion, Austin, TX) and stored at -20°C until use.

2.4.2 Quantitative Real-time PCR (qPCR) Analysis

To quantify mRNA expression levels, RT-qPCR was performed using a Viia™ 7 thermocycler (Applied Biosystems, California). The specificity of the qPCR products was assessed at the end of the reactions by analyzing the dissociation curves. TOP2B

and ACTB for PCLS samples, and GAPDH and PPIA for HepG2 cells were selected for their stable expression upon treatments, assessed with NormFinder software (Andersen et al., 2004), and used as reference genes. Non-reverse transcribed RNA was used as non-template control (NTC) for verification of the genomic DNA amplification signal. Data from qPCR were analyzed with the LinRegPCR 2016 program enabling the determination of the starting concentrations (N0) based on the observed PCR efficiency values. mRNA expression levels in samples exposed to DON were expressed relative to the mean of the control (Maruo et al., 2018).

Table 2: Table of human primer sequences used for RT-qPCR analysis (F: Forward; R: Reverse).

Gene symbol	Gene name	Primer sequence	mRNA	References
FOS	AP-1 Transcription Factor Subunit	F: ACGCGCAGGACTTCTGCAC R: GAATGAAGTTGGCACTGGAGAC	AH003773.2	Present study
ATF3	Activating Transcription Factor 3	F: GGCGACGAGAAAGAAATAAG R: CAGCTTCTCCGACTCTTT	NM_001674.4	Present study
HNF4	Hepatocyte Nuclear Factor 4 Alpha	F: CAGATGATCGAGCAGATCCA R: CGTTGGTTCCCATATGTTCC	X76930.1	Present study
CASP3	Caspase 3	F: GAGGCCGACTTCTTGTAT R: CAAAGCGACTGGATGAAC	NM_004346.4	Present study
CASP 9	Caspase 9	F: CACACCCAGTGACATCTTT R: AGGGTCTCAACGTACCA	AB020979.1	Present study
CAT	Catalase	F: CTTCGACCCAAGCAACAT R: GGGACAGTTCACAGGTATATG	NM_001752.4	Present study
SOD2	Superoxide Dismutase 2	F: GGTTGGCTTGGTTTCAATAAG R: GTGCTCCCACACATCAAT	NM_000636.4	Present study
HMOX1	Heme Oxygenase 1	F: CAGGCAGAGGGTGATAGA R: CTCCTGCAACTCCTCAAAG	NM_002133	Present study
IL8	Interleukin 8	F: GATTTCTGCAGCTCTGTG R: GTGGAAAGGTTTGGAGTATG	NM_000584	Present study
TNFα	Tumor Necrosis Factor Alpha	F: CCTGTAGCCCATGTTGTA R: CCAGCTGGTTATCTCTCA	NM_000594	Present study
NF-κβ	Nuclear Factor Kappa B	F: GAGCAACCTAAACAGAGAGG R: TTGACCTGAGGGTAAGACT	NM_003998.4	Present study
CCL20	C-C Motif Chemokine Ligand 20	F: GGCTGCTTTGATGTCAGT R: GAAGAATACGGTCTGTGTATCC	NM_001130046.2	Present study
PPIA	Peptidylprolyl Isomerase A	F: GTCAACCCCACCGTGTTCTTC R: TTTCTGCTGTCTTTGGGACCTTG	ENST00000355968	Present study
GAPDH	Glyceraldehyde-3-Phosphate Dehydrogenase	F: TCAAGGCTGAGAACGGGAAG R: CCACTTGATTTTGGAGGGATCTC	NM_002046	Luo et al., 2021

Table 3: Table of pig primer sequences used for RT-qPCR analysis (F: Forward; R: Reverse).

Gene symbol	Gene name	Primer sequence	mRNA	References
FOS	AP-1 Transcription Factor Subunit	F: CACTGTGAACAGATCAGC R: GAAGTCGGTCAGTTCTTTC	ENSSSCT00000014174.4	Present study
ATF3	Activating Transcription Factor 3	F: TGAGGTTCGCCATCCA R: TACCTCGGCTTTCGTGA	ENSSSCT00000033171.2	Present study
HNF4	Hepatocyte Nuclear Factor 4 Alpha	F: TACTGCAGGCTCAAGAAGTG R: CTGCTATCCTCGTAGCTTGAC	NM_001044571.1	Present study
IL1α	Interleukin 1 Alpha	F: GCCAATGACACAGAAGAAGA R: ATGCACTGGTGGTTGATG	NM_214029	Pierron et al., 2022
IL8	Interleukin 8	F: GCTCTCTGTGAGGCTGCAGTTC R: AAGGTGTGGAATGCGTATTTATGC	NM_213867	Grenier et al., 2011
TNFα	Tumor necrosis factor alpha	F: ACTGCACTTCGAGGTTATCGG R: GGCGACGGGCTTATCTGA	NM_214022	Cano et al. 2013
NF-κβ	Nuclear Factor Kappa β	F: CCTCCACAAGGCAGCAAATAG R: TCCACACCGCTGTCACAGA	ENSSSCT00000033438	Alassane-Kpembi et al, 2017a
CCL20	C-C Motif Chemokine Ligand 20	F: GCTCCTGGCTGCTTTGATGTC R: CATTGGCGAGCTGCTGTGTG	NM_001024589	Meurens et al., 2009
ACTB	Actin β	F: GCACCACACCTTCTACA R: ATCTGGGTCATCTTCTCAC	ENSSSCT00000008324.1	Present study
TOP2B	DNA Topoisomerase II Beta	F: AAGGGCGAGAGGTCAATGAT R: ACATCTTCTCGTTCTTGCGC	ENSSSCT00015080370.1	Park et al., 2015

2.5 Statistical analysis

All statistical analyses were performed using GraphPad Prism 9.0.2 software (GraphPad Software Inc., La Jolla, USA). Data are expressed as mean ± SEM (standard error of the mean). Significant differences were assessed by one-way ANOVA followed by Tukey's test for cytotoxicity and by the unpaired Student's t-test for parametric data and Mann Whitney test for non-parametric data for all the other analyses. p-value≤0.05 was considered statistically significant.

3. RESULTS

3.1 Effects of DON on HepG2 cells

DON cytotoxicity was first evaluated on human liver cells (Figure 1). After 4 h exposure to DON, the viability of HepG2 cells decreased significantly at concentrations of 6.25 µM (12% reduction) to 100 µM (17% reduction). After 24 h, viability decreased after

DON exposure from 0.8 (9% reduction) to 100 µM (40% reduction). DON showed higher cytotoxic effects after 48 h exposure from 1.6 to 100 µM (15% and 50% inhibition, respectively).

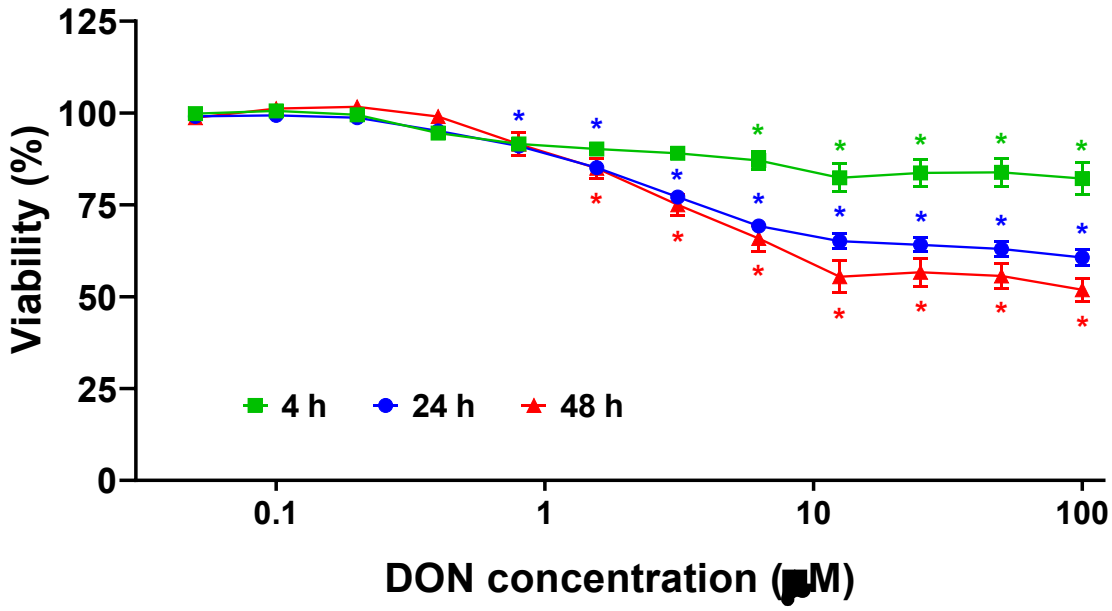

Figure 1. Toxicity of DON in HepG2 cells evaluated by measurement of the reducing potential of cells (RealTime-Glo™ MT Cell Viability Assay) after 4 h, 24 h, and 48 h. Cell viability is expressed as % of control cells. Data are presented as mean ± SEM of six replicates, *p ≤ 0.05.

To complete the analysis of the hepatic toxicity of DON, the abundance of genes involved in apoptosis, inflammation and oxidative stress were evaluated by RT-qPCR.

The liver is exposed to a multitude of xenobiotics, including mycotoxins. Being the primary target tissue and main metabolizer of many xenobiotics, it is very sensitive to tissue injury leading to cell apoptosis. We thus evaluated the expression of genes involved in apoptosis. We observed that the expression of caspase-3 (CASP3) and caspase-9 (CASP9) increased in HepG2 exposed to DON (2.7- and 1.4-fold, respectively) (Figure 2).

Besides its metabolic role, the liver is also a key tissue involved in the immune system (Kubes and Jenne, 2018). For this reason, we also assessed the expression of cytokine genes. Upon exposure to DON, increased expression of interleukin 8 (IL8) (16.6-fold), tumor necrosis factor α (TNFα) (17.6-fold) and the C-C motif chemokine ligand 20 (CCL20) (8.8-fold) was observed, but no changes in interleukin 1α (IL1α) (Figure 2). The expression of the transcription factor nuclear factor-kappa B (NF-κB) (4.7-fold), which controls the transcription of many inflammatory cytokines, was also found to be up-regulated upon exposure to DON (Figure 2). Similarly, the Fos proto-oncogene (FOS) (66.8-fold), the expression of activating transcription factor 3 (ATF3) (28.7-fold) and of hepatocyte nuclear factor 4 α (HNF4) (1.3-fold) were increased upon exposure to DON (Figure 2).

DON, like other mycotoxins, can induce oxidative stress in the liver. Thus, the last set of tested genes concerned enzymes involved in oxidative stress. In HepG2 cells, a significant increase (2.2-fold) only in the catalase (CAT) and superoxide dismutase 2 (SOD2) (2.5-fold) genes, and a (0.7-fold) decrease in heme oxygenase 1 (HMOX1) were observed (Figure 2).

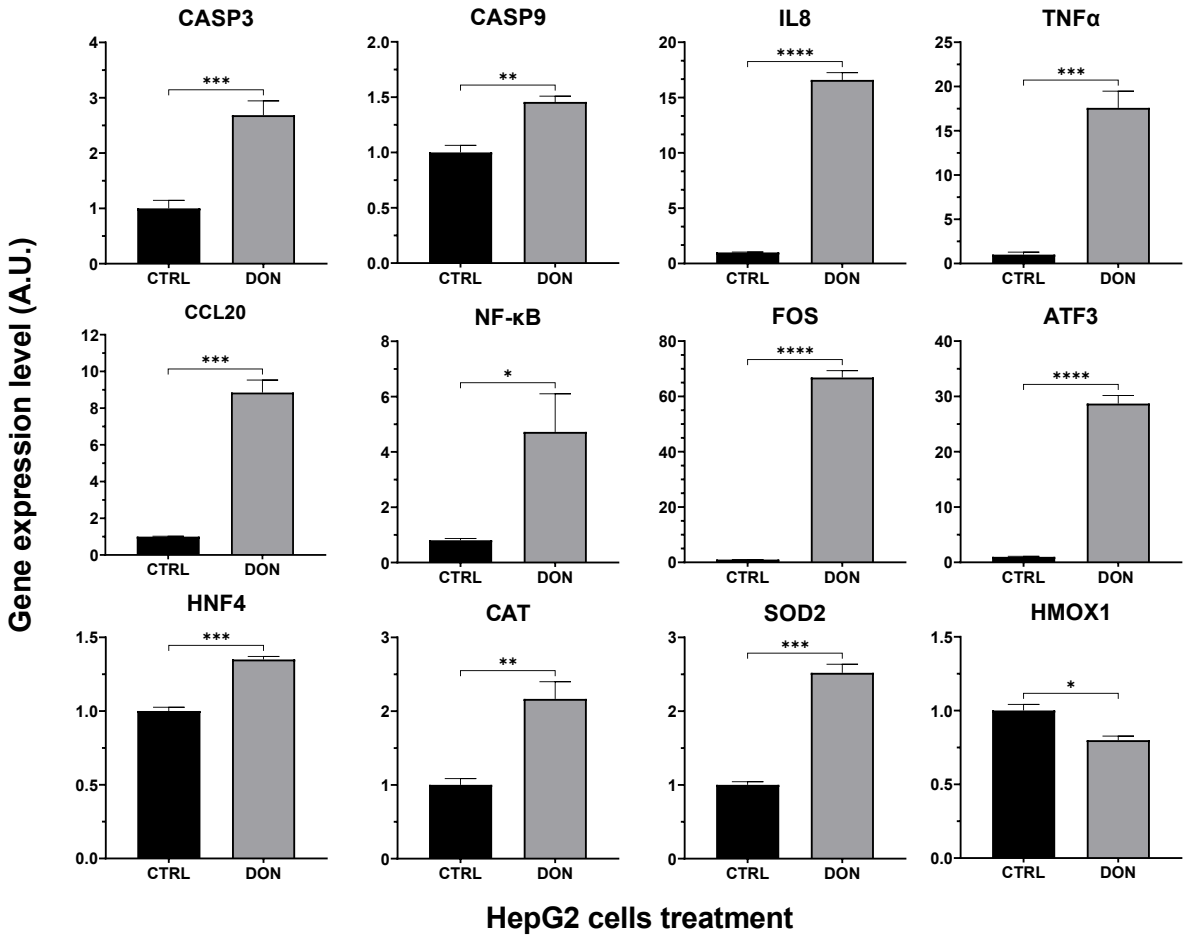

Figure 2. Apoptosis, inflammatory, transcription factors and oxidative stress mRNA levels measured by RT-PCR in HepG2 cells exposed or not to 10 µM DON for 4 h. Data are presented as mean ± SEM of six replicates, **p ≤ 0.01, **p ≤ 0.01, ***p ≤ 0.001 and ****p ≤ 0.0001.

3.2 Effects of DON on PCLS

To not limit our observations to a hepatic cell line, experiments were also performed on porcine PCLS. This later model has the advantage to include all liver cell types within the context of a preserved hepatic architecture, including the conservation of intercellular and cell-matrix interactions (de Graaf et al., 2010).

The hepatic effects of DON were first assessed histologically. A significant increase in the lesion score was observed in DON-treated PCLS ($p \leq 0.001$). The main histological changes in PCLS were disorganization of hepatic cords, apoptosis and cytoplasmic vacuolation of hepatocytes (Figure 3). Despite tissue damages, we observed no significant increase in biomarkers of liver injury (alanine transaminase - ALT, aspartate aminotransferase – AST and lactate dehydrogenase - LDH), cholestasis (alkaline phosphatase - ALP), or hepatic function (total proteins) in the PCLS supernatant upon DON treatment (Supplementary data - Table S1).

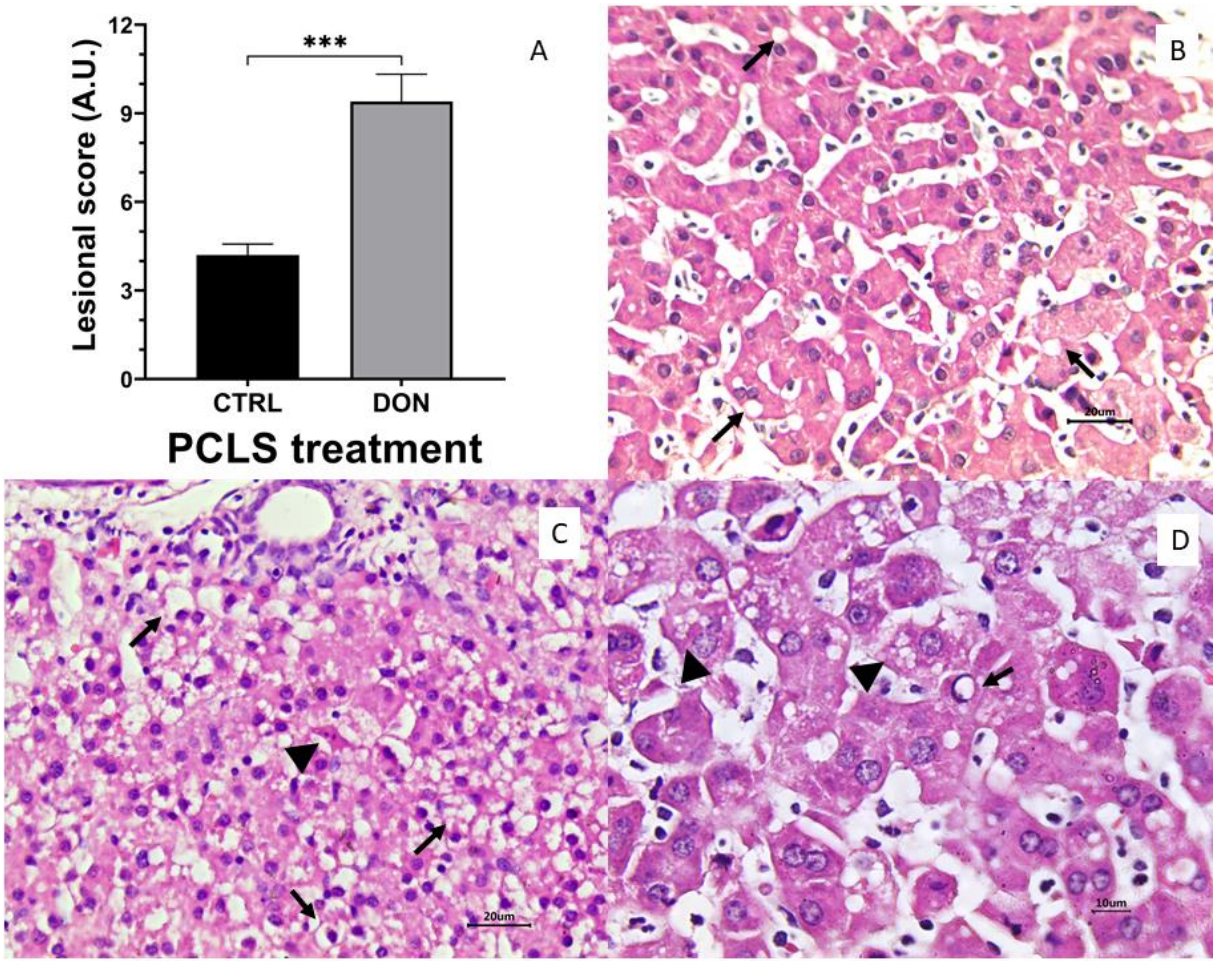

Figure 3. Effects of 4 h DON exposure on PCLS. A- Lesion score (A.U. – arbitrary units). Data are presented as mean ± SEM of five different animals, ***p ≤ 0.001. B- control group. Mild disorganization of hepatocytes trabeculae and cytoplasmic vacuolation (arrows). HE. Scale bar 20 µm. C – DON group. Moderate cytoplasmic vacuolation of hepatocytes (arrows) and apoptosis (arrowhead). HE. Scale bar 20 µm. D- DON group. Cytoplasmic vacuolation (arrowheads) and nuclear vacuolation (arrows) of hepatocytes. HE. Scale bar 10 µm.

Because apoptosis was an important histological finding in DON-exposed PCLS, we sought to confirm activation of a cysteine protease, caspase-3 (CASP3), a key effector in cell apoptosis. A significant increase in CASP3 immunostaining was observed in the treated group (p ≤ 0.01) compared to the control (Figure 4). The brownish immunostaining was randomly distributed in hepatocytes and Kupffer cells.

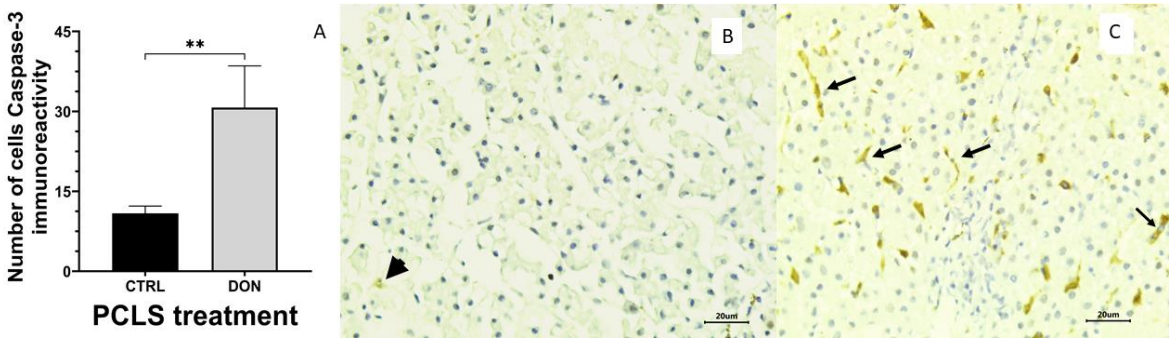

Figure 4. Analysis of apoptosis in PCLS. A- Mean number of immunoreactive cells for CASP3 in PCLS/field. Data are presented as mean ± SEM of five different animals), **p ≤ 0.01. B–C- Immunoperoxidase staining. B- control group. Mild positive CASP3 staining (arrowhead). Scale bar 20 µm. C- DON group. Moderate CASP3 positive staining in hepatocytes and Kupffer cells (arrows). Scale bar 20 µm.

Next, we investigated the effect of DON on gene expression. As already observed in HepG2 cells, exposure of PCLS to 10 µM DON stimulates the expression of IL8 (8-fold), TNFα (17.2-fold), and CCL20 (7.4-fold) (Figure 5). In these samples, DON also induced the expression of IL1α (8.9-fold). Like in HepG2 cells, DON was found to upregulate the transcription factors NF-κB, FOS, and ATF3 (2.9-, 5-, and 3-fold, respectively) in PCLS (Figure 5).

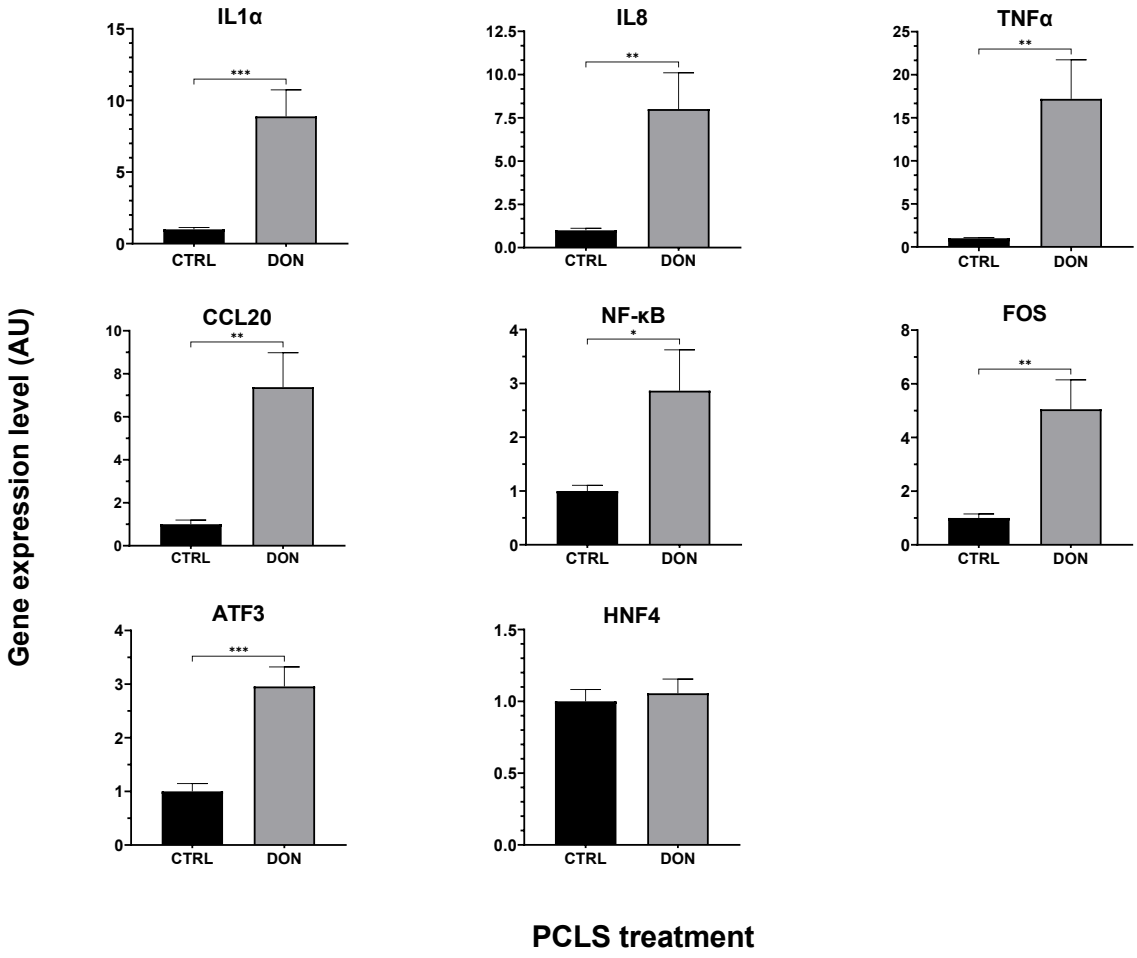

Figure 5. Inflammatory and transcription factors mRNA levels measured by RT-PCR in PCLS exposed or not to DON for 4 h. Data are mean ± SEM from 9 different animals. *p ≤ 0.05, **p ≤ 0.01, and ***p ≤ 0.001.

By contrast, in PCLS, no significant differences were observed in the expression of any of the oxidative stress genes analyzed (data not shown).

4. DISCUSSION

Many studies have reported an effect of DON on the intestine and the lymphoid organs (Luo et al., 2019; Novak et al., 2021; Pinton and Oswald, 2014), but investigations on the impact of DON on the liver are scarcer. The present study evaluated the effects of DON on liver tissue, particularly PCLS. The human hepatocyte cell line, HepG2, was used for comparison.

Due to the difficulties in accessing human liver samples, the study was performed on porcine PCLS. The pig is considered a good model for extrapolation to humans (Helke and Swindle, 2013). PCLS retain the original three-dimensional structure of the liver, preserve hepatocytes and Kupffer cells as well as cellular crosstalk and cell-matrix interactions (De Graaf et al., 2010). PCLS thus appear to be highly suitable for studies of the toxic effects of food contaminants. This model has two main advantages, (i) cultured explants is in line with 3R principles, as one animal allows the assessment of multiple doses and (ii) it gives access to a fully differentiated three-dimensional model for histopathology assessment. A few studies using rat PCLS have addressed the effects of mycotoxins, one assessed the effect of fumonisin B1 on sphingoid base (Norred et al., 1996), another one the impact of aflatoxins on RNA synthesis (Friedman et al., 1997), and a third one described the metabolization of *Alternaria* toxins into potentially toxic compounds (Burkhardt et al., 2011).

A cytotoxic effect of DON was observed in HepG2 cells at low concentrations (0.8-1.6 µM), regardless of the duration of exposure (4, 24, and 48 h). The decrease observed at these low concentrations after 24 h is in agreement with the results of previous

studies (Darwish et al., 2020; Mayer et al., 2017) indicating that short exposure to realistic doses of DON alters hepatic cells.

Damages to the tissue were observed in PCLS exposed to DON, despite the short time of exposure (4 h), but no changes in markers of liver function or injury. Thus, histology can be considered a sensitive endpoint for liver damage. In PCLS, disorganization of hepatic cords, apoptosis and cytoplasmic vacuolation of hepatocytes were observed after 4 h of exposure to 10 µM DON. These histological changes are similar to those obtained in subchronic *in vivo* trials. Indeed, disorganization of hepatic cords, apoptosis, cytoplasmic and nuclear vacuolation of hepatocytes, megalocytosis and focal necrosis were observed in piglets or gilts fed diets contaminated with 0.012 to 3 mg/kg DON for one to six weeks (Bracarense et al., 2020; Gerez et al., 2015; Grenier et al., 2011; Pierron et al., 2018; Skiepko et al., 2020).

The cytoplasmic vacuolation observed in PCLS may be related to the DON-induced impairment of mitochondrial function (Springler et al., 2017). Indeed, mitochondrial dysfunction leads to failure of the Na^+/K^+-ATPase pump causing an influx of Na^+, Ca^{+2}, and water into the cytosol, inducing, cytoplasmic vacuolation (Miller and Zachary, 2017). Moreover, an increased number of apoptotic hepatocytes and cells in hepatic sinusoids was observed in gilts exposed to a fusariotoxins-contaminated diet (Dolenšek et al., 2021).

Apoptosis observed in PCLS was confirmed by immunostaining of CASP3. Liver apoptosis has already been reported in piglets injected intravenously with DON (Mikami et al., 2010) as well as in mice and pigs fed a DON-contaminated diet (Bracarense et al., 2017; Gerez et al., 2015; Sun et al., 2014). Apoptosis can occur via different pathways (Elmore, 2007). The extrinsic pathway induced by transmembrane

death-receptor interactions activates CASP8 and subsequently CASP3. The intrinsic or mitochondrial pathway involves intracellular signals such as p53, resulting in the activation of CASP9 and subsequently of CASP3 (van Cruchten and van den Broeck, 2002). In the present study, we observed upregulation of both CASP3 and CAPS9. CASP9 activation suggests that in the liver the intrinsic pathway is involved in DON-induced apoptosis, as already demonstrated in the intestine (Payros et al., 2021b). In the same way, as observed for the histological evaluation of PCLS exposed to DON, it should be noted that the evaluation of apoptosis has revealed similar effects to those observed *in vivo* in different species.

DON is known to activate the inflammatory response. Indeed, DON-induced ribotoxic stress leads to the activation of the MAPK1/2 pathway, which in turn activates several immediate-early genes and induces the production of cytokines, the expression of cyclooxygenase-2 (COX2), and apoptosis (Pestka, 2010a; Pierron et al., 2016) in different target organs (Payros et al., 2016; Pestka, 2010a). In the present study, we observed overexpression of various cytokines in both HepG2 cells and PCLS. Such pro-inflammatory expression patterns have already been observed in the liver of pigs and rats fed a DON-contaminated diet (Abdel-Wahhab et al., 2015; Chen et al., 2008). In our study, IL1α gene expression was only upregulated in PCLS. This difference might be due to the presence of Kupffer cells in hepatic tissue that are known to produce high levels of this cytokine (Bilzer et al., 2006) in the liver (Bai et al., 2021). The IL1α was also shown to be expressed in the intestine after *in vivo* exposure to DON (Pestka, 2010b). Taken together, these results show that pro-inflammatory cytokines are sensitive markers when the liver is exposed to DON and that such inflammation can be observed *in vitro* (hepatocytes), *ex vivo* (PCLS), and *in vivo*.

Concerning transcription factors, DON-activation of MAPK pathway activates immediate-early genes, such as FOS and ATF3, in turn promoting the expression of COX2, cytokines and apoptosis (Nielsen et al., 2009; Smith et al., 2017b; Sun et al., 2015; Yuan et al., 2018). In the present study, we demonstrated an increase in the expression of FOS, ATF3 in PCLS and of HNF4 only, in HepG2 cells. ATF3 reveals endoplasmic reticulum (ER) stress. In absence of relieve of ER, cells can go into apoptosis (Holtz et al., 2006; Li et al., 2006). FOS is highly induced in HepG2 cells, probably due to its stabilization by sustained extracellular signal-regulated kinase (ERK) signaling (Murphy et al., 2002). In HepG2 cells, but not in PCLS, we observed increased expression of HNF4, a transcription factor that controls the expression of several hepatic-specific genes involved in hepatic metabolism (Madec et al., 2011; Petrescu et al., 2002). The cancerous origin of HepG2 cells, which implies different demands as regard on metabolic processes (Coller, 2014), could explain the high induction of these transcription factors.

5. CONCLUSION

We observed that short exposure to DON reduces HepG2 cells viability and induces toxic effects on hepatic cells and liver tissue. In particular, we demonstrated that in accordance with the effects observed in pigs fed a DON-contaminated-diet, this toxin induces the expression of genes involved in liver apoptosis and inflammation and histological damages.

To the best of our knowledge, this is the first to use PCLS for the identification of DON toxic effects on liver structure and functions. .

Pig PCLS is a promising model to study the effects of DON, and potentially other mycotoxins on the liver. It enables the demonstration of histomorphological and molecular effects at realistic dietary levels, in very good accordance with data obtained

in *in vivo* trials. As pig is a good model for extrapolation to humans and is very sensitive to mycotoxins, particularly to DON, our results are relevant for progressing towards a better assessment of human consumers risk related to mycotoxins.

Supplementary data: Table S1. Effects of DON exposure (10 µM) on hepatic biomarkers in PCLS supernatant

Author Contributions: "Conceptualization, A.L.H, P.P., A.P.B, and I.P.O.; methodology, P.P., A.L.H., A.K., E.P. S.B.; validation, A.L.H., S.P., and A.K.; formal analysis, A.L.H., P.P., and A.P.B.; investigation, A.L.H., A.P.B, P.P., A.K., S.P., S.B. and E.P.; resources, A.P.B. and P.P.; data curation, A.L.H. and P.P.; writing—original draft preparation, A.L.H.; writing—review and editing, A.L.H, A.P.B., P.P., and I.P.O.; visualization, A.L.H. and P.P.; supervision, A.P.B and I.P.O.; project administration, A.L.H, P.P.; funding acquisition, A.P.B., I.P.O., and P.P. All authors have read and agreed to the published version of the manuscript."

Funding: A.L.H received a fellowship from the Coordenação de Aperfeiçoamento de Pessoal de Nível Superior-CAPES/Cofecub, grant number 0389/2019. This research was supported by the ANR grant "EmergingMyco" (ANR-18-CE34-0014).

Acknowledgments: The authors would like to express their gratitude to the residents and Ricardo L. N. de Matos in the Laboratory of Animal Pathology (UEL) for their practical support during histological analyses, to Mikael Albin (INRAE-Toxalim) for animal experiment phases and to Claire Naylies and Yannick Lippi for their contribution to qPCR experiments performed at GeT-TRiX Genopole Toulouse Midi-Pyrénées facility.

Conflicts of Interest: The authors have no conflict of interest to declare

6. REFERENCES

Abdel-Wahhab, M.A., El-Kady, A.A., Hassan, A.M., Abd El-Moneim, O.M., Abdel-Aziem, S.H., 2015. Effectiveness of Activated Carbon and Egyptian Montmorillonite in the Protection Against Deoxynivalenol-induced Cytotoxicity and Genotoxicity in Rats. Food and Chemical Toxicology 83, 174–182. https://doi.org/10.1016/j.fct.2015.06.015

Alassane-Kpembi, I., Gerez, J.R., Cossalter, A.-M., Neves, M., Laffitte, J., Naylies, C., Lippi, Y., Kolf-Clauw, M., Bracarense, A.P.L., Pinton, P., Oswald, I.P., 2017a. Intestinal Toxicity of the Type B Trichothecene Mycotoxin Fusarenon-X: Whole Transcriptome Profiling Reveals New Signaling Pathways. Scientific Reports 7, 7530. https://doi.org/10.1038/s41598-017-07155-2

Alassane-Kpembi, I., Puel, O., Pinton, P., Cossalter, A.-M., Chou, T.-C., Oswald, I.P., 2017b. Co-exposure to low doses of the food contaminants deoxynivalenol and nivalenol has a synergistic inflammatory effect on intestinal explants. Archives of Toxicology 91, 2677–2687. https://doi.org/10.1007/s00204-016-1902-9

Andersen, C.L., Jensen, J.L., Ørntoft, T.F., 2004. Normalization of Real-Time Quantitative Reverse Transcription-PCR Data: A Model-Based Variance Estimation Approach to Identify Genes Suited for Normalization, Applied to Bladder and Colon Cancer Data Sets. Cancer Research 64, 5245–5250. https://doi.org/10.1158/0008-5472.CAN-04-0496

Bai, Y., Ma, K., Li, Jibo, Li, Jianping, Bi, C., Shan, A., 2021. Deoxynivalenol exposure induces liver damage in mice: Inflammation and immune responses, oxidative stress, and protective effects of Lactobacillus rhamnosus GG. Food and Chemical Toxicology 156, 112514. https://doi.org/10.1016/j.fct.2021.112514

Bilzer, M., Roggel, F., Gerbes, A.L., 2006. Role of Kupffer Cells in Host Defense and Liver Disease. Liver International 26, 1175–1186. https://doi.org/10.1111/j.1478-3231.2006.01342.x

Bracarense, A.P.F.L., Basso, K.M., da Silva, E.O., Payros, D., Oswald, I.P., 2017. Deoxynivalenol in the Liver and Lymphoid Organs of Rats: Effects of Dose and Duration on Immunohistological Changes. World Mycotoxin Journal 10, 89–96. https://doi.org/10.3920/WMJ2016.2094

Bracarense, A.P.F.L., Lucioli, J., Grenier, B., Drociunas Pacheco, G., Moll, W.D., Schatzmayr, G., Oswald, I.P., 2012. Chronic ingestion of deoxynivalenol and fumonisin, alone or in interaction, induces morphological and immunological changes in the intestine of piglets. British Journal of Nutrition 107, 1776–1786. https://doi.org/10.1017/S0007114511004946

Bracarense, A.P.F.L., Pierron, A., Pinton, P., Gerez, J.R., Schatzmayr, G., Moll, W.D., Zhou, T., Oswald, I.P., 2020. Reduced Toxicity of 3-epi-deoxynivalenol and De-epoxy-deoxynivalenol through Deoxynivalenol Bacterial Biotransformation: In Vivo Analysis in Piglets. Food and Chemical Toxicology 140, 111241. https://doi.org/10.1016/j.fct.2020.111241

Burkhardt, B., Wittenauer, J., Pfeiffer, E., Schauer, U.M.D., Metzler, M., 2011. Oxidative metabolism of the mycotoxins alternariol and alternariol-9-methyl ether in precision-cut rat liver slices in vitro. Molecular Nutrition & Food Research 55, 1079–1086. https://doi.org/10.1002/mnfr.201000487

Chen, F., Ma, Y., Xue, C., Ma, J., Xie, Q., Wang, G., Bi, Y., Cao, Y., 2008. The combination of Deoxynivalenol and Zearalenone at Permitted Feed Concentrations Causes Serious Physiological Effects in Young Pigs. Journal of Veterinary Science 9, 39. https://doi.org/10.4142/jvs.2008.9.1.39

Coller, H.A., 2014. Is Cancer a Metabolic Disease? The American Journal of Pathology 184, 4–17. https://doi.org/10.1016/j.ajpath.2013.07.035

Darwish, W.S., Chen, Z., Li, Y., Tan, H., Chiba, H., Hui, S.-P., 2020. Deoxynivalenol-induced alterations in the redox status of HepG2 cells: identification of lipid hydroperoxides, the role of Nrf2-Keap1

signaling, and protective effects of zinc. Mycotoxin Research 36, 287–299. https://doi.org/10.1007/s12550-020-00392-x

de Graaf, I.A.M., Olinga, P., de Jager, M.H., Merema, M.T., de Kanter, R., van de Kerkhof, E.G., Groothuis, G.M.M., 2010. Preparation and incubation of precision-cut liver and intestinal slices for application in drug metabolism and toxicity studies. Nature Protocols 5, 1540–1551. https://doi.org/10.1038/nprot.2010.111

Dewyse, L., Reynaert, H., van Grunsven, L.A., 2021. Best Practices and Progress in Precision-Cut Liver Slice Cultures. International Journal of Molecular Sciences 22, 7137. https://doi.org/10.3390/ijms22137137

Dolenšek, T., Švara, T., Knific, T., Gombač, M., Luzar, B., Jakovac-Strajn, B., 2021. The Influence of Fusarium Mycotoxins on the Liver of Gilts and Their Suckling Piglets. Animals 11, 2534. https://doi.org/10.3390/ani11092534

Elmore, S., 2007. Apoptosis: A Review of Programmed Cell Death. Toxicologic Pathology 35, 495–516. https://doi.org/10.1080/01926230701320337

Eskola, M., Kos, G., Elliott, C.T., Hajšlová, J., Mayar, S., Krska, R., 2020. Worldwide contamination of food-crops with mycotoxins: Validity of the widely cited 'FAO estimate' of 25%. Critical Reviews in Food Science and Nutrition 60, 2773–2789. https://doi.org/10.1080/10408398.2019.1658570

Fernández-Blanco, C., Elmo, L., Waldner, T., Ruiz, M., 2018. Cytotoxic Effects Induced by Patulin, Deoxynivalenol and Toxin T2 Individually and in Combination in Hepatic Cells (HepG2). Food and Chemical Toxicology 120, 12–23. https://doi.org/10.1016/j.fct.2018.06.019

Friedman, L., Gaines, D.W., Chi, R.K., Smith, M.C., Braunberg, R.C., Thorpe, C.W., 1997. INTERACTION OF AFLATOXINS AS MEASURED BY THEIR BIOCHEMICAL ACTION ON RAT LIVER SLICES AND HEPATOCYTES. Toxic Substance Mechanisms 16, 15–42. https://doi.org/10.1080/107691897229775

Gerez, J.R., Camacho, T., Brunaldi Marutani, V.H., Nascimento de Matos, R.L., Hohmann, M.S., Verri Júnior, W.A., Bracarense, A.P.F.R.L., 2021. Ovarian toxicity by fusariotoxins in pigs: Does it imply in oxidative stress? Theriogenology 165, 84–91. https://doi.org/10.1016/j.theriogenology.2021.02.003

Gerez, J.R., Desto, S.S., Bracarense, A.P.F.R.L., 2017. Deoxynivalenol induces toxic effects in the ovaries of pigs: An ex vivo approach. Theriogenology 90, 94–100. https://doi.org/10.1016/j.theriogenology.2016.10.023

Gerez, J.R., Pinton, P., Callu, P., Grosjean, F., Oswald, I.P., Bracarense, A.P.F.L., 2015. Deoxynivalenol Alone or in Combination with Nivalenol and Zearalenone Induce Systemic Histological Changes in Pigs. Experimental and Toxicologic Pathology 67, 89–98. https://doi.org/10.1016/j.etp.2014.10.001

Grenier, B., Bracarense, A.-P.F.L., Schwartz, H.E., Trumel, C., Cossalter, A.-M., Schatzmayr, G., Kolf-Clauw, M., Moll, W.-D., Oswald, I.P., 2012. The low intestinal and hepatic toxicity of hydrolyzed

fumonisin B1 correlates with its inability to alter the metabolism of sphingolipids. Biochemical Pharmacology 83, 1465–1473. https://doi.org/10.1016/j.bcp.2012.02.007

Grenier, B., Loureiro-Bracarense, A.-P., Lucioli, J., Pacheco, G.D., Cossalter, A.-M., Moll, W.-D., Schatzmayr, G., Oswald, I.P., 2011. Individual and Combined Effects of Subclinical Doses of Deoxynivalenol and Fumonisins in Piglets. Molecular Nutrition & Food Research 55, 761–771. https://doi.org/10.1002/mnfr.201000402

Helke, K.L., Swindle, M.M., 2013. Animal models of toxicology testing: the role of pigs. Expert Opinion on Drug Metabolism & Toxicology 9, 127–139. https://doi.org/10.1517/17425255.2013.739607

Holtz, W.A., Turetzky, J.M., Jong, Y.-J.I., O'Malley, K.L., 2006. Oxidative stress-triggered unfolded protein response is upstream of intrinsic cell death evoked by parkinsonian mimetics. Journal of Neurochemistry 99, 54–69. https://doi.org/10.1111/j.1471-4159.2006.04025.x

Kasper, H.-U., Dries, V., Drebber, U., Kern, M.A., Dienes, H.P., Schirmacher, P., 2005. Precision cut tissue slices of the liver as morphological tool for investigation of apoptosis. In vivo (Athens, Greece) 19, 423–31.

Knutsen, H.K., Alexander, J., Barregård, L., Bignami, M., Brüschweiler, B., Ceccatelli, S., Cottrill, B., Dinovi, M., Grasl-Kraupp, B., Hogstrand, C., Hoogenboom, L. (Ron), Nebbia, C.S., Oswald, I.P., Petersen, A., Rose, M., Roudot, A., Schwerdtle, T., Vleminckx, C., Vollmer, G., Wallace, H., de Saeger, S., Eriksen, G.S., Farmer, P., Fremy, J., Gong, Y.Y., Meyer, K., Naegeli, H., Parent-Massin, D., Rietjens, I., van Egmond, H., Altieri, A., Eskola, M., Gergelova, P., Ramos Bordajandi, L., Benkova, B., Dörr, B., Gkrillas, A., Gustavsson, N., van Manen, M., Edler, L., 2017. Risks to human and animal health related to the presence of deoxynivalenol and its acetylated and modified forms in food and feed. EFSA Journal 15. https://doi.org/10.2903/j.efsa.2017.4718

Kubes, P., Jenne, C., 2018. Immune Responses in the Liver. Annual Review of Immunology 36, 247–277. https://doi.org/10.1146/annurev-immunol-051116-052415

Li, J., Lee, B., Lee, A.S., 2006. Endoplasmic Reticulum Stress-induced Apoptosis. Journal of Biological Chemistry 281, 7260–7270. https://doi.org/10.1074/jbc.M509868200

Luo, S., Terciolo, C., Bracarense, A.P.F.L., Payros, D., Pinton, P., Oswald, I.P., 2019. In Vitro and In Vivo Effects of a Mycotoxin, Deoxynivalenol, and a Trace Metal, Cadmium, Alone or in a Mixture on the Intestinal Barrier. Environment International 132, 105082. https://doi.org/10.1016/j.envint.2019.105082

Luo, S., Terciolo, C., Neves, M., Puel, S., Naylies, C., Lippi, Y., Pinton, P., Oswald, I.P., 2021. Comparative sensitivity of proliferative and differentiated intestinal epithelial cells to the food contaminant, deoxynivalenol. Environmental Pollution 277, 116818. https://doi.org/10.1016/j.envpol.2021.116818

Madec, S., Cerec, V., Plée-Gautier, E., Antoun, J., Glaise, D., Salaun, J.-P., Guguen-Guillouzo, C., Corlu, A., 2011. CYP4F3B Expression Is Associated with Differentiation of HepaRG Human Hepatocytes and Unaffected by Fatty Acid Overload. Drug Metabolism and Disposition 39, 1987–1996. https://doi.org/10.1124/dmd.110.036848

Maresca, M., Pinton, P., Ajandouz, E.H., Menard, S., Ferrier, L., Oswald, I.P., 2018. Overview and Comparison of Intestinal Organotypic Models, Intestinal Cells, and Intestinal Explants Used for Toxicity Studies, in: Current Topics in Microbiology and Immunology. Springer Science and Business Media Deutschland GmbH, pp. 247–264. https://doi.org/10.1007/82_2018_142

Maruo, V., Bracarense, A.P.F.R.L., Metayer, J.-P., Vilarino, M., Oswald, I., Pinton, P., 2018. Ergot Alkaloids at Doses Close to EU Regulatory Limits Induce Alterations of the Liver and Intestine. Toxins 10, 183. https://doi.org/10.3390/toxins10050183

Mayer, E., Novak, B., Springler, A., Schwartz-Zimmermann, H.E., Nagl, V., Reisinger, N., Hessenberger, S., Schatzmayr, G., 2017. Effects of Deoxynivalenol (DON) and its Microbial Biotransformation Product Deepoxy-deoxynivalenol (DOM-1) on a Trout, Pig, mouse, and Human Cell Line. Mycotoxin Research 33, 297–308. https://doi.org/10.1007/s12550-017-0289-7

Mikami, O., Yamaguchi, H., Murata, H., Nakajima, Y., Miyazaki, S., 2010. Induction of Apoptotic Lesions in Liver and Lymphoid Tissues and Modulation of Cytokine mRNA Expression by Acute Exposure to Deoxynivalenol in Piglets. Journal of Veterinary Science 11, 107–113. https://doi.org/10.4142/jvs.2010.11.2.107

Miller, M.A., Zachary, J.F., 2017. Mechanisms and Morphology of Cellular Injury, Adaptation, and Death, in: Zachary, J.F. (Ed.), Pathologic Basis of Veterinary Disease. Elsevier, St. Louis, pp. 2-43.e19. https://doi.org/10.1016/B978-0-323-35775-3.00001-1

Murphy, L.O., Smith, S., Chen, R.-H., Fingar, D.C., Blenis, J., 2002. Molecular interpretation of ERK signal duration by immediate early gene products. Nature Cell Biology 4, 556–564. https://doi.org/10.1038/ncb822

Narváez, A., Castaldo, L., Izzo, L., Pallarés, N., Rodríguez-Carrasco, Y., Ritieni, A., 2022. Deoxynivalenol contamination in cereal-based foodstuffs from Spain: Systematic review and meta-analysis approach for exposure assessment. Food Control 132, 108521. https://doi.org/10.1016/j.foodcont.2021.108521

Nielsen, C., Lippke, H., Didier, A., Dietrich, R., Märtlbauer, E., 2009. Potential of deoxynivalenol to induce transcription factors in human hepatoma cells. Molecular Nutrition & Food Research 53, 479–491. https://doi.org/10.1002/mnfr.200800475

Norred, W.P., Riley, R.T., Meredith, F.I., Bacon, C.W., Voss, K.A., 1996. Time- and dose-response effects of the mycotoxin, fumonisin B1 on sphingoid base elevations in precision-cut rat liver and kidney slices. Toxicology in Vitro 10, 349–358. https://doi.org/10.1016/0887-2333(96)00013-6

Novak, B., Hasuda, A.L., Ghanbari, M., Mayumi Maruo, V., Bracarense, A.P.F.R.L., Neves, M., Emsenhuber, C., Wein, S., Oswald, I.P., Pinton, P., Schatzmayr, D., 2021. Effects of Fusarium metabolites beauvericin and enniatins alone or in mixture with deoxynivalenol on weaning piglets. Food and Chemical Toxicology 158, 112719. https://doi.org/10.1016/j.fct.2021.112719

Oliveira, M.S., Rocha, A., Sulyok, M., Krska, R., Mallmann, C.A., 2017. Natural Mycotoxin Contamination of Maize (Zea mays L.) in the South Region of Brazil. Food Control 73, 127–132. https://doi.org/10.1016/j.foodcont.2016.07.033

Palma, E., Doornebal, E.J., Chokshi, S., 2019. Precision-cut liver slices: a versatile tool to advance liver research. Hepatology International 13, 51–57. https://doi.org/10.1007/s12072-018-9913-7

Payros, D., Alassane-Kpembi, I., Laffitte, J., Lencina, C., Neves, M., Bracarense, A.P., Pinton, P., Ménard, S., Oswald, I.P., 2021a. Dietary Exposure to the Food Contaminant Deoxynivalenol Triggers Colonic Breakdown by Activating the Mitochondrial and the Death Receptor Pathways. Molecular Nutrition & Food Research 2100191. https://doi.org/10.1002/mnfr.202100191

Payros, D., Alassane-Kpembi, I., Pierron, A., Loiseau, N., Pinton, P., Oswald, I.P., 2016. Toxicology of deoxynivalenol and its acetylated and modified forms. Archives of Toxicology 90, 2931–2957. https://doi.org/10.1007/s00204-016-1826-4

Payros, D., Garofalo, M., Pierron, A., Soler-Vasco, L., Al-Ayoubi, C., Maruo, V.M., Alassane-Kpembi, I., Pinton, P., Oswald, I.P., 2021b. Les mycotoxines en alimentation humaine : un défi pour la recherche. Cahiers de Nutrition et de Diététique 56, 170–183. https://doi.org/10.1016/j.cnd.2021.02.001

Pestka, J.J., 2010a. Deoxynivalenol-Induced Proinflammatory Gene Expression: Mechanisms and Pathological Sequelae. Toxins 2, 1300–1317. https://doi.org/10.3390/toxins2061300

Pestka, J.J., 2010b. Deoxynivalenol: mechanisms of action, human exposure, and toxicological relevance. Archives of Toxicology 84, 663–679. https://doi.org/10.1007/s00204-010-0579-8

Petrescu, A.D., Hertz, R., Bar-Tana, J., Schroeder, F., Kier, A.B., 2002. Ligand Specificity and Conformational Dependence of the Hepatic Nuclear Factor-4α (HNF-4α). Journal of Biological Chemistry 277, 23988–23999. https://doi.org/10.1074/jbc.M201241200

Pierron, A., Bracarense, A.P.F.L., Cossalter, A.M., Laffitte, J., Schwartz-Zimmermann, H.E., Schatzmayr, G., Pinton, P., Moll, W.D., Oswald, I.P., 2018. Deepoxy-deoxynivalenol Retains Some Immune-modulatory Properties of the Parent Molecule Deoxynivalenol in Piglets. Archives of Toxicology 92, 3381–3389. https://doi.org/10.1007/s00204-018-2293-x

Pierron, A., Mimoun, S., Murate, L.S., Loiseau, N., Lippi, Y., Bracarense, A.P.F.L., Liaubet, L., Schatzmayr, G., Berthiller, F., Moll, W.D., Oswald, I.P., 2016. Intestinal toxicity of the masked mycotoxin deoxynivalenol-3-β-d-glucoside. Archives of Toxicology 90, 2037–2046. https://doi.org/10.1007/s00204-015-1592-8

Pierron, A., Neves, M., Puel, S., Lippi, Y., Soler, L., Miller, J.D., Oswald, I.P., 2022. Intestinal toxicity of the new type A trichothecenes, NX and 3ANX. Chemosphere 288, 132415. https://doi.org/10.1016/j.chemosphere.2021.132415

Pinton, P., Accensi, F., Beauchamp, E., Cossalter, A.M., Callu, P., Grosjean, F., Oswald, I.P., 2008. Ingestion of Deoxynivalenol (DON) Contaminated Feed Alters the Pig Vaccinal Immune Responses. Toxicology Letters 177, 215–222. https://doi.org/10.1016/j.toxlet.2008.01.015

Pinton, P., Oswald, I.P., 2014. Trichothecenes on the Intestine : A Review. Toxins 6, 1615–1643. https://doi.org/10.3390/toxins60

Robert, H., Payros, D., Pinton, P., Théodorou, V., Mercier-Bonin, M., Oswald, I.P., 2017. Impact of mycotoxins on the intestine: are mucus and microbiota new targets? Journal of Toxicology and Environmental Health, Part B 20, 249–275. https://doi.org/10.1080/10937404.2017.1326071

Ruan, F., Chen, J.G., Chen, L., Lin, X. tian, Zhou, Y., Zhu, K. jing, Guo, Y.T., Tan, A.J., 2020. Food Poisoning Caused by Deoxynivalenol at a School in Zhuhai, Guangdong, China, in 2019. Foodborne Pathogens and Disease 17, 429–433. https://doi.org/10.1089/fpd.2019.2710

Silva, E.O. da, Gerez, J.R., Drape, T. do C., Bracarense, A.P.F.R.L., 2014. Phytic Acid Decreases Deoxynivalenol and Fumonisin B1-Induced Changes on Swine Jejunal Explants. Toxicology Reports 1, 284–292. https://doi.org/10.1016/j.toxrep.2014.05.001

Silva, E.O. da, Gerez, J.R., Hohmann, M.S.N., Verri, W.A., Bracarense, A.P.F.R.L., 2019. Phytic Acid Decreases Oxidative Stress and Intestinal Lesions Induced by Fumonisin B1 and Deoxynivalenol in Intestinal Explants of Pigs. Toxins 11, 18. https://doi.org/10.3390/toxins11010018

Skiepko, N., Przybylska-Gornowicz, B., Gajęcka, M., Gajęcki, M., Lewczuk, B., 2020. Effects of Deoxynivalenol and Zearalenone on the Histology and Ultrastructure of Pig Liver. Toxins 12, 463. https://doi.org/10.3390/toxins12070463

Smith, M.-C., Hymery, N., Troadec, S., Pawtowski, A., Coton, E., Madec, S., 2017a. Hepatotoxicity of fusariotoxins, alone and in combination, towards the HepaRG human hepatocyte cell line. Food and Chemical Toxicology 109, 439–451. https://doi.org/10.1016/j.fct.2017.09.022

Smith, M.-C., Madec, S., Pawtowski, A., Coton, E., Hymery, N., 2017b. Individual and Combined Toxicological Effects of Deoxynivalenol and Zearalenone on Human Hepatocytes in In Vitro Chronic Exposure Conditions. Toxicology Letters 280, 238–246. https://doi.org/10.1016/j.toxlet.2017.08.080

Souza, M. de, Baptista, A.A.S., Valdiviezo, M.J.J., Justino, L., Menck-Costa, M.F., Ferraz, C.R., da Gloria, E.M., Verri, W.A., Bracarense, A.P.F.R.L., 2020. Lactobacillus spp. Reduces Morphological Changes and Oxidative Stress Induced by Deoxynivalenol on the Intestine and Liver of Broilers. Toxicon 185, 203–212. https://doi.org/10.1016/j.toxicon.2020.07.002

Springler, A., Hessenberger, S., Reisinger, N., Kern, C., Nagl, V., Schatzmayr, G., Mayer, E., 2017. Deoxynivalenol and its metabolite deepoxy-deoxynivalenol: multi-parameter analysis for the evaluation of cytotoxicity and cellular effects. Mycotoxin Research 33, 25–37. https://doi.org/10.1007/s12550-016-0260-z

Starokozhko, V., Abza, G.B., Maessen, H.C., Merema, M.T., Kuper, F., Groothuis, G.M.M., 2015. Viability, Function and Morphological Integrity of Precision-cut Liver Slices During Prolonged Incubation: Effects of Culture Medium. Toxicology in Vitro 30, 288–299. https://doi.org/10.1016/j.tiv.2015.10.008

Sun, L.-H., Lei, M., Zhang, N.-Y., Gao, X., Li, C., Krumm, C.S., Qi, D.-S., 2015. Individual and combined cytotoxic effects of aflatoxin B1, zearalenone, deoxynivalenol and fumonisin B1 on BRL 3A rat liver cells. Toxicon 95, 6–12. https://doi.org/10.1016/j.toxicon.2014.12.010

Sun, L.H., Lei, M.Y., Zhang, N.Y., Zhao, L., Krumm, C.S., Qi, D.S., 2014. Hepatotoxic effects of mycotoxin combinations in mice. Food and Chemical Toxicology 74, 289–293. https://doi.org/10.1016/j.fct.2014.10.020

Terciolo, C., Maresca, M., Pinton, P., Oswald, I.P., 2018. Review article: Role of satiety hormones in anorexia induction by Trichothecene mycotoxins. Food and Chemical Toxicology 121, 701–714. https://doi.org/10.1016/j.fct.2018.09.034

van Cruchten, S., van den Broeck, W., 2002. Morphological and Biochemical Aspects of Apoptosis, Oncosis and Necrosis. Anatomia, Histologia, Embryologia: Journal of Veterinary Medicine Series C 31, 214–223. https://doi.org/10.1046/j.1439-0264.2002.00398.x

Vin, K., Rivière, G., Leconte, S., Cravedi, J.-P., Fremy, J.M., Oswald, I.P., Roudot, A.-C., Vasseur, P., Jean, J., Hulin, M., Sirot, V., 2020. Dietary exposure to mycotoxins in the French infant total diet study. Food and Chemical Toxicology 140, 111301. https://doi.org/10.1016/j.fct.2020.111301

Wu, X., Roberto, J.B., Knupp, A., Kenerson, H.L., Truong, C.D., Yuen, S.Y., Brempelis, K.J., Tuefferd, M., Chen, A., Horton, H., Yeung, R.S., Crispe, I.N., 2018. Precision-cut human liver slice cultures as an immunological platform. Journal of Immunological Methods 455, 71–79. https://doi.org/10.1016/j.jim.2018.01.012

Yuan, L., Mu, P., Huang, B., Li, H., Mu, H., Deng, Y., 2018. EGR1 is essential for deoxynivalenol-induced G2/M cell cycle arrest in HepG2 cells via the ATF3ΔZip2a/2b-EGR1-p21 pathway. Toxicology Letters 299, 95–103. https://doi.org/10.1016/j.toxlet.2018.09.012

Zhang, X., Jiang, L., Geng, C., Cao, J., Zhong, L., 2009. The Role of Oxidative Stress in Deoxynivalenol-induced DNA Damage in HepG2 Cells. Toxicon 54, 513–518. https://doi.org/10.1016/j.toxicon.2009.05.021

Author Contributions: “Conceptualization, A.L.H, P.P., A.P.B, and I.P.O.; methodology, P.P., A.L.H., A.K., E.P. S.B.; validation, A.L.H., S.P., and A.K.; formal analysis, A.L.H., P.P., and A.P.B.; investigation, A.L.H., A.P.B, P.P., A.K., S.P., S.B. and E.P.; resources, A.P.B. and P.P.; data curation, A.L.H. and P.P.; writing—original draft preparation, A.L.H.; writing—review and editing, A.L.H, A.P.B., P.P., and I.P.O.; visualization, A.L.H. and P.P.; supervision, A.P.B and I.P.O.; project administration, A.L.H, P.P.; funding acquisition, A.P.B., I.P.O., and P.P. All authors have read and agreed to the published version of the manuscript.”

HIGHLIGHTS

- Liver is a target organ for deoxynivalenol (DON)
- DON induces inflammation and apoptosis in HepG2 cells and pig precision-cut liver slices (PCLS)
- Histomorphological and molecular effects in PCLS are similar to *in vivo* observations
- Precision liver slices are a relevant model for assessing the toxicity of mycotoxins
- Extrapolation of pig PCLS data to humans may be useful for consumers risk assessment

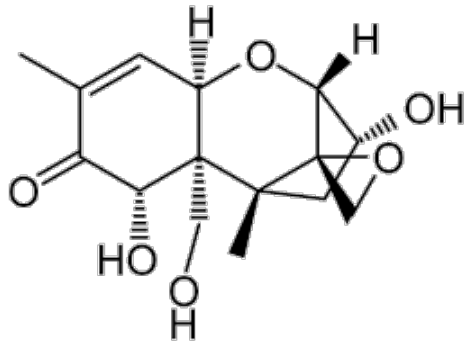

Deoxynivalenol

Liver

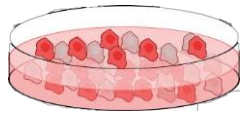

cultured cells (HepG2)

Effects on inflammation, apoptosis and oxidative stress

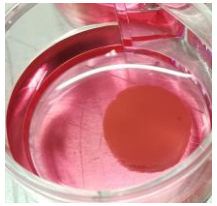

liver slices

Effects on histomorphology, inflammation and apoptosis

A promising model for studying hepatotoxicity of food contaminants, in line with 3R principles

in vivo trials

Effects on histomorphology, inflammation and apoptosis

(literature review)

Deoxynivalenol induces apoptosis and inflammation in the liver: analysis using precision-cut liver slices

Amanda Lopes Hasuda[1,2*], Elodie Person[2], Abdullah Khoshal[2], Sandrine Bruel[2], Sylvie Puel[2], Isabelle P. Oswald[2*], Ana Paula F. R. L. Bracarense[1], Philippe Pinton[2]

[1] Laboratory of Animal Pathology, Universidade Estadual de Londrina, P.O. Box 10.011, Londrina, PR 86057-970, Brazil; amanda.lopeshasuda@uel.br (A.L.H.) anapaula@uel.br (A.P.B.)

[2] Toxalim (Research Centre in Food Toxicology), University of Toulouse, INRAE, ENVT, INP-Purpan, UPS, 31027, Toulouse, France; elodie.person@inrae.fr (E.P.), a.khoshal@outlook.com (A.K.), sandrine.bruel@inrae.fr (S.B.), sylvie.puel@inrae.fr (S.P.); isabelle.oswald@inrae.fr (I.P.O.); philippe.pinton@inrae.fr (P.P.)

[*]Corresponding authors: amanda.lopeshasuda@uel.br, isabelle.oswald@inrae.fr

Supplementary data

Table S1. Effects of DON exposure (10µM) on hepatic biomarkers in PCLS supernatant (mean ± SEM).

Hepatic biomarkers	**Control**	**DON**
Alkaline phosphatase (U/L)	4.393±1.599	3.687±1.892
Alanine transaminase (U/L)	6.333±4.885	6.500±2.811
Aspartate aminotransferase (U/L)	260.8±153.6	278.2±99.23
Lactate dehydrogenase (U/L)	83.02±40.27	100.3±47.71
Total proteins (g/L)	5.707±0.573	6.311±0.452